MRS Advances © 2016 Materials Research Society
DOI: 10.1557/adv.2016.544

Thin film bi-epitaxy and transition characteristics of TiO_2/TiN buffered VO_2 on Si(100) substrates

Adele Moatti[1], Reza Bayati[2], Srinivasa Rao Singamaneni[1], Jagdish Narayan[1]

1. Department of Materials Science and Engineering, North Carolina State University, EB-1, Raleigh, NC 27695-7906, USA
2. Intel Corporation, RA_3, Hillsboro, OR 97124, USA

ABSTRACT

Bi-epitaxial VO_2 thin films with [011] out-of-plane orientation were integrated with Si(100) substrates through TiO_2/TiN buffer layers. At the first step, TiN is grown epitaxially on Si(100), where a cube-on-cube epitaxy is achieved. Then, TiN was oxidized in-situ ending up having epitaxial r-TiO_2. Finally, VO_2 was deposited on top of TiO_2. The alignment across the interfaces was stablished as $VO_2(011)\|TiO_2(110)\|TiN(100)\|Si(100)$ and $VO_2(110)/VO_2(010)\|TiO_2(011)\|TiN(112)\|Si(112)$. The inter-planar spacing of $VO_2(010)$ and $TiO_2(011)$ equal to 2.26 and 2.50 Å, respectively. This results in a 9.78% tensile misfit strain in $VO_2(010)$ lattice which relaxes through 9/10 alteration domains with a frequency factor of 0.5, according to the domain matching epitaxy paradigm. Also, the inter-planar spacing of $VO_2(011)$ and $TiO_2(011)$ equals to 3.19 and 2.50 Å, respectively. This results in a 27.6% compressive misfit strain in $VO_2(011)$ lattice which relaxes through 3/4 alteration domains with a frequency factor of 0.57. We studied semiconductor to metal transition characteristics of VO_2/TiO_2/TiN/Si heterostructures and established a correlation between intrinsic defects and magnetic properties.

INTRODUCTION

Combination of semiconducting and magnetic properties has led to development of spintronic (spin based electronics). This achievement facilitates production of spin-based devices. Different materials have been investigated for this application and some semiconductors such as VO_2, ZnO, TiO_2, Y_2O_3, and In_2O_3 have shown promising results at room temperature [1-5]. Among those VO_2 shows a strong correlated electron system with a small band gap (~0.7 eV at room temperature) but its magnetic properties have not been studied yet. VO_2 can serve as a smart material which generally responds to temperature, pressure variations and electric or magnetic fields. It is worth mentioning that VO_2 has semiconductor-to-metal transition (SMT) at about 340 K resulting from an ultrafast phase transformation from a high temperature tetragonal state to a low temperature monoclinic state [6-8].

Considering practical applications, there is a problem with the bulk VO_2 that it cannot withstand the repeated thermal cycling, while thin films and nanoparticles are more inclined to tolerate these stresses. Also, the SMT for films and nanoparticles can be tuned to room temperature, which makes their application very unique, such as, thermally activated optical switching [9,10], thermal relays and energy management devices [11,12], infrared sensors and actuators [13], micro-bolometers [14,15], electrochromic and photochromic memory and optical devices [16,17]. Magnetic, electrical, and optical properties of semiconductors are controlled through native defects. Also, they play a role in diffusion mechanism involved in growth, processing, and device degradation. Point defects affect electrical and optical properties of semiconductors. These point defects consist of intrinsic native defects i.e. vacancies, interstitials, impurities, and defect complexes.

In this study, we provide a new platform of TiO_2/TiN to grow bi-epitaxial VO_2 while integrated with Si(100). This paper focuses on the epitaxial relations across the interfaces. Metal to semiconductor transition for VO_2 are investigated and discussed. We report the magnetic properties of the VO_2 thin film and the role of defects in defining and tuning these properties is discussed.

EXPERIMENTAL DETAILS

The VO_2/TiO_2/TiN/Si thin film heterostructures were grown on Si(100) substrates employing pulsed laser deposition (PLD). A Lambda Physik (LPX200) KrF excimer laser, with λ=248 nm, t=25 ns, and the average power of 2.5 W was used to ablate the targets. The laser gas composition was 0.12% F_2, 2.22% He, 4.6% Kr, and 92.94% Ne. The laser beam was incident at an angle of 45° on the surface of the targets which were rotated during the deposition to provide uniform ablation characteristics of the target surface. The energy density and repetition rate were set at 3-3.5 J.cm^{-2} and 5 Hz. The TiN buffer was deposited at 920 K for 4000 pulses under 10^{-5} Torr using a high density 99.9% pure TiN target. Through 2 min oxidation under oxygen pressure of 10^{-2} Torr, half of TiN epilayer was oxidized to TiO_2 at 920 K [18]. The VO_2 layer was then deposited at 720 K under an oxygen pressure of 10^{-2} Torr for 3000 pulses. The VO_2 target was made by sintering 99.5 % pure VO_2 powder under Ar atmosphere at 1100 °C for 12 h.

A Rigaku diffractometer with Cu-Kα radiation (λ=0.154 nm) was used to study the out-of-plane orientation of the films. A Philips X'Pert Pro diffractometer was employed for φ-scan XRD to confirm in-plane alignment and epitaxial growth characteristics across the interfaces. Transmission Kikuchi Diffraction (TKD) mapping was carried out on FEI Quanta Focused Ion Beam. Sample was prepared by Focused Ion Beam (FIB), The FEI Quanta 3D FEG to be transparent to electron beam for TKD technique. The sample with pressed indium dots was mounted on a custom built rotatable pogo-pin setup in the PPMS. The magnetic measurements were done using Quantum design Super-conducting Quantum Interference Device (SQUID).

DISCUSSION

Figure 1 shows the theta-2theta scan of X-Ray diffraction pattern of VO_2 thin film grown on the Si(100) substrate buffered with TiO_2/TiN layers. The pattern represented either a highly textured or an epitaxial VO_2 layer with the out of plane orientation of (011). Thus, the out of plane relationship can be established as $VO_2(011) \| TiO_2(110) \| TiN(100) \| Si(100)$. In order to investigate the in-plane orientation relationship, ϕ scan of X-Ray diffraction pattern (Figure 2) were performed on different reflection of the planes. The results reveal a cube-on-cube growth as for the TiN and Si crystals by DME paradigm. Four sharp φ-signals from {111} family of planes of TiO_2 originate from (111) and $(\bar{1}\bar{1}1)$ planes for $(110)/(\bar{1}\bar{1}0)$ as well as $(1\bar{1}1)$ and $(\bar{1}11)$ planes for $(1\bar{1}0)/(\bar{1}10)$ of titania. The common direction between TiO_2\{110\} and TiO_2\{111\} planes is $<\bar{1}10>$ which has an azimuthal rotation of 45° with respect to TiN<100> axis. The (101) reflection of VO_2 layer shows 8 peaks with intervals of 22.5° angular separation from each other. The common direction between VO_2\{101\} and VO_2\{011\} planes is $<\bar{1}\bar{1}1>$ which has an azimuthal rotation of 22.5° with respect to Si<100> and TiO_2<110> axis.

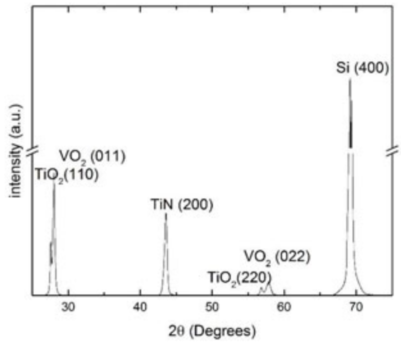

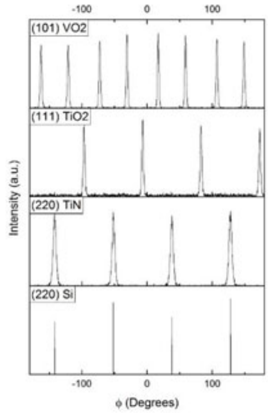

Figure 1. XRD θ-2θ pattern acquired from the VO_2(011)/TiO_2 (110)/TiN(100)/Si (100) heterostructure

Figure 2. Results of XRD φ-scan preformed on the VO_2(011)/TiO_2(110)/TiN(100)/Si(100) heterostructure: Si(220) reflection, TiN(220) reflection, TiO_2(111) reflection, and VO_2(101) reflection

For additional details of alignment across interfaces, TKD data were collected from these heterostructures. Figure 3a represents the cross section electron image of the VO_2(011)/TiO_2(110)/TiN(100)/Si(100) heterostructures with the thickness of 110, 100, and 315 nm, for TiN, TiO_2, and VO_2 layers respectively. The band contrast image is displayed in Figure 3b which shows where crystallographic direction has a major change. As it is clear in VO_2 layer there are vertical grain boundaries illustrating different directions. Figure 3c depicts VO_2/TiO_2/TiN/Si heterostructure's phase map and Figure 3d provides a pole figure map of layers. The Si and TiN have similar Kikuchi, also TiO_2 layer is so thin that makes it hard to detect with this technique. Inverse pole figure map also confirms there are two major colors in VO_2 layer suggesting two major orientations for observed grains. According to orientation map, two epitaxial relationships are established as VO_2(010) and VO_2(110)‖TiO_2(011)‖TiN(112)‖Si(112). Figure 4 a, b, and c & d show the Kikuchi patterns of Si, TiN, TiO_2, and two orientation of VO_2 respectively. These patterns also confirm the cube on cube alignment of Si and TiN. Also patterns of TiO_2 and VO_2 are in accordance with established relationship of VO_2(110)‖TiO_2(011) and VO_2(010)‖TiO_2(011). The orientations in VO_2 grains as represented in Figure 5 alternate between (010) and (110). The presence of two types of grains with different orientations explains the appearance of eight peaks in phi-scan XRD with four peaks belongs to each plane. The inter-planar spacing of VO_2(010) and TiO_2(011) equal to 2.26 and 2.50 Å, respectively. The mentioned matching results in a 9.78% tensile misfit strain in VO_2(010) lattice which relaxes through 9/10 and 10/11 alteration domains with a frequency factor of 0.5, according to the domain matching epitaxy paradigm [19]. Also, the inter-planar spacing of VO_2(011) and TiO_2(011) equal to 3.19 and 2.50 Å, respectively. This results in a

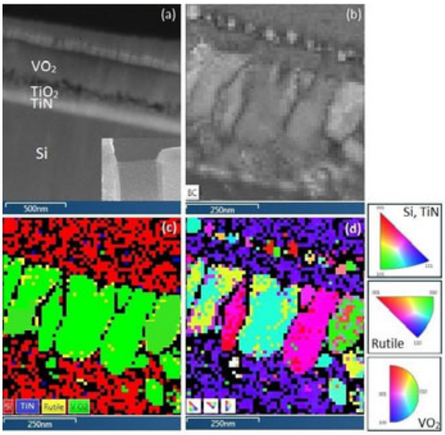

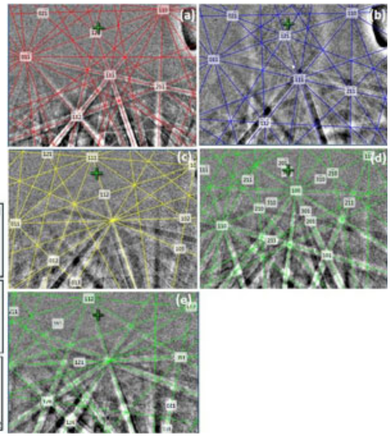

Figure 3. TKD result of the FIB slice (a) Cross section electron image and the FIB made sample at the right corner, (b) Band contrast image, (c) Phase map image, and (d) Inverse pole figure map (IPF Y) of interfaces acquired from the VO_2(011)/TiO_2 (110)/TiN(100)/Si (100) heterostructure

Figure 4. Kikuchi patterns of (a) Si, (b) TiN, (c) TiO_2, and (d, e) VO_2 layers

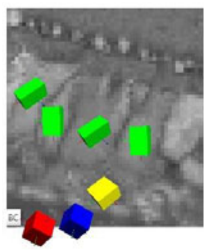

Figure 5. Poles belong to each layer of Si, TiN, TiO_2, and VO_2 in the cross section band contrast image, respectively from bottom to top

27.6% compressive misfit strain in VO_2(011) lattice which relaxes through 2/3 and 3/4 alteration domains with a frequency factor of 0.57.

Figure 6 displays the semiconductor to metal transition (SMT) temperature of VO_2/TiO_2/TiN/Si heterostructure. Sharp transition in the heterostructure was observed with amplitude of over 5 orders of magnitude. The hysteresis is about 8 K and transition temperature is 350 K.

Magnetic properties of these films were measured by sweeping magnetic field from -600 to 600 Oe at three different temperatures of 4, 100, and 300 K. The hysteresis loops are shown in Figure 7. It is interesting to note the presence of ferromagnetism in VO_2 thin film. The presence of ferromagnetism is attributed to oxygen vacancy and reduction of Vanadium from V^{4+} to V^{3+}. In fact, the formation of oxygen vacancies is accompanied by the release of electrons to the lattice which is subsequently trapped by V^{4+} cations to preserve charge neutrality. This phenomenon results in the formation of V^{3+} cations. The formation of oxygen vacancies and V^{3+} species can be explained by the following reaction:

$$2VO_2 \rightarrow V_2O_3 + V_O^{''} + 2e^- \qquad (1)$$

Where $V_O^{''}$ represents an oxygen vacancy. This reaction stipulates that the non-stoichiometric VO_2 thin films have a higher charge carrier concentration (e^-) and must exhibit a lower resistivity in the semiconducting state [7]. Ferromagnetic behavior in other heterostructure including VO_2 has been observed previously by our group [20].

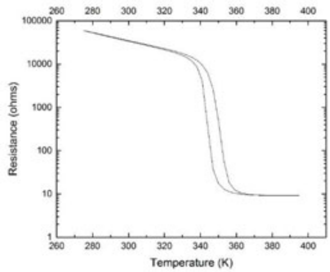

Figure 6. Resistance versus temperature in $VO_2/TiO_2/TiN/Si$ heterostructure

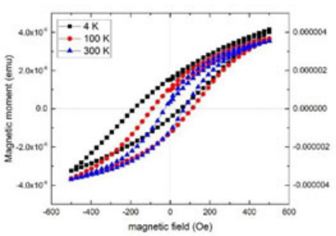

Figure 7. Magnetic field dependent magnetization of $VO_2(011)$ measurement at 4, 100, and 300 K with 200 Oe field cooling

CONCLUSION

In this paper, we have successfully integrated VO_2 thin film on Si through buffer layer of TiO_2/TiN. The TiN were grown cube-on-cube on Si, and TiO_2 was oxidized epitaxially with [110] out-of-plane orientation. VO_2 was then deposited on TiO_2 with out-of-plane direction parallel to [011]. The in-plane relationship established to be $VO_2(110)/VO_2(010) \| TiO_2(011) \| TiN(112) \| Si(112)$ based on transmission Kikuchi Diffraction. Metal to semiconductor transition was defined to be 350 K with 8 K hysteresis, according to resistance versus temperature hysteresis loop. We have observed the ferromagnetic behavior in VO_2 samples and argued that it is due to the formation of oxygen vacancies or V^{3+} defects with unpaired electrons. Therefore, the formation of oxygen vacancies or non-stoichiometric oxidation state of vanadium in VO_2, is envisaged to be responsible for the observed room-temperature ferromagnetic characteristics.

ACKNOWLEDGMENTS

This research was supported by NSF grant DMR-1304607. The authors acknowledge the use of the Analytical Instrumentation Facility (AIF) at North Carolina State University, which is supported by the State of North Carolina and the National Science Foundation.

REFERENCES

[1] Mal S, Nori S, Narayan J, Prater JT. J.Mater.Res. 2011;26:1298.
[2] Mal S, Yang T, Gupta P, Prater J, Narayan J. Acta materialia 2011;59:2526.
[3] Park C, Yoon S, Jo Y, Shin S. 2009
[4] Wu C, Huang S, Lee W, Chang Y, Wu T, Soo Y et al. Appl.Phys.Lett. 2012;101:162403.
[5] Zhao Y, Motapothula M, Yakovlev N, Liu Z, Dhar S, Rusydi A et al. Appl.Phys.Lett. 2012;101:142105.
[6] Ramanathan S. Harvard University: Springer New York Dordrecht Heidelberg London 2010
[7] Morin F. Phys.Rev.Lett. 1959;3:34.
[8] Narayan J, Bhosle V. J.Appl.Phys. 2006;100:3524.
[9] Becker, MF, Buckman, AB, Walser, RM, Lepine, T, Georges, PM, Brun, A. 1994:400.
[10] Soltani M, Chaker M, Haddad E, Kruzelecky R, Margot J. Journal of Vacuum Science & Technology A 2007;25:971.
[11] Soltani M, Chaker M, Haddad E, Kruzelesky R. Journal of Vacuum Science and Technology.A, International Journal Devoted to Vacuum, Surfaces, and Films 2006;24
[12] Manning TD, Parkin IP, Clark RJ, Sheel D, Pemble ME, Vernadou D. Journal of Materials Chemistry 2002;12:2936.
[13] Rajendra Kumar R, Karunagaran B, Mangalaraj D, Narayandass SK, Manoravi P, Joseph M et al. Sensors and Actuators A: Physical 2003;107:62.
[14] Chen C, Yi X, Zhao X, Xiong B. Sensors and Actuators A: Physical 2001;90:212.
[15] Reintsema, CD, Grossman, EN, Koch, JA. 1999:190.
[16] Chivian JS, Scott MW, Case WE, Krasutsky NJ. Quantum Electronics, IEEE Journal of 1985;21:383.
[17] Ko C, Ramanathan S. J.Appl.Phys. 2008;104:6105.
[18] Moatti A, Bayati R, Narayan J. Acta Materialia 2016;103:502.
[19] Narayan J, Larson B. J.Appl.Phys. 2003;93:278.
[20] Molaei R, Bayati R, Nori S, Kumar D, Prater J, Narayan J. Appl.Phys.Lett. 2013;103:252109.